Monobiotinylated Proteins Tethered to Microspheres for Detection of Antigen-Specific Serum Antibodies

Caleb S. Whitley, Thomas C. Mitchell*

Department of Microbiology and Immunology, University of Louisville School of Medicine, 505 S. Hancock St., Louisville KY 40202

*Corresponding author: Thomas C. Mitchell, E-mail: thomas.mitchell@louisville.edu. Clinical and Translational Research Building, 505 South Hancock Street, Louisville, KY, 40202

ABSTRACT

Surface modified microspheres have been leveraged as a useful way to immobilize antigen for serological studies. The use of carboxyl modified microspheres for this purpose is well-established, but commonly associated with technical challenges. Streptavidin modified microspheres require little technical expertise and thus address some of the short-comings of carboxyl microspheres. An additional feature of streptavidin microspheres is the use of mono-biotinylated proteins, which contain a single biotinylation motif at the C-terminus. However, the relative performance of streptavidin and carboxyl microspheres is unknown. Here, we performed a head-to-head comparison of streptavidin and carboxyl microspheres. We compared antigen binding, orientation, and staining quality and found that both microspheres perform similarly based on these defined parameters. We also evaluated the utility of streptavidin microspheres bound to severe acute respiratory syndrome coronavirus 2 (SARS-CoV-2) receptor binding domain (RBD), to reliably detect RBD-specific IgG1, IgG3, and IgA1 produced in individuals recently immunized with Pfizer/BioNTech mRNA coronavirus disease (COVID) vaccine as 'proof-of-concept'. We provide evidence that each of the antibody targets are detectable in serum using RBD-coated microspheres, Ig-specific 'detector' monoclonal antibodies (mAbs), and flow cytometry. We found that cross-reactivity of the detector mAbs can be minimized by antibody titration to improve differentiation between IgG1 and IgG3. We also coated streptavidin microspheres with SARS-CoV-2 delta variant RBD to determine if the streptavidin microsphere approach revealed any differences in binding of immune serum antibodies to wild-type (Wuhan) versus variant RBD (Delta). Overall, our results show that streptavidin microspheres loaded with mono-biotinylated antigen is a robust alternative to chemically cross-linking antigen to carboxyl microspheres for use in serological assays.

Keywords: COVID, microspheres, serology, vaccine, variant

INTRODUCTION

The use of microspheres as solid supports for serological studies is well-established [1-3]. However, the performance of different microsphere modifications, such as carboxyl versus streptavidin, has yet to be evaluated. Carboxyl (COOH) modified microspheres are increasingly used for serological assays because they can be covalently bound with protein antigens of interest [2,4,5]. These bonds are formed between activated carboxyl groups on the microspheres and amine groups present in varying numbers on the surfaces of most proteins; *i.e.* amino acid residues with free amines in their side chains (lysine, arginine, asparagine, and glutamine). However, use of these amino acid residues as attachment sites could theoretically destroy or alter epitopes recognized by immune serum antibodies. Moreover, multiple cross-linking sites on a protein likely results in its coupling to COOH microspheres in a variety of orientations that are disorganized, which could complicate serological studies.

An additional potential drawback of COOH microspheres is variability of cross-linking efficiencies due to low stability of some of the conjugation reagents involved [6]. Loading streptavidin (SA) microspheres with commercially available biotinylated

proteins provides an alternative. Biotinylation of proteins is typically achieved by cross-linking biotin to proteins using the same chemistry as that of COOH microsphere conjugation, such that the same amino acid residues, with free amines, are used to biotinylate proteins. Thus, loading SA microspheres with multi-biotinylated proteins under these conditions avoids the need for cross-linking chemistry by the end user, but it does not solve the potential problems of epitope destruction and disorganized orientation relative to a physiological target (*e.g.* a viral particle with symmetric surface epitopes).

A more physiological approach is to use protein antigens engineered to contain a single biotinylation motif recognized by the biotin ligase BirA [7]. Co-expression of BirA in human embryonic kidney cells 293 (HEK293) cells in which the recombinant protein being expressed allows production of protein antigens with a single biotin, and a human-specific glycosylation pattern [8]. An increasing number of recombinant proteins are commercially available with mono-biotinylated 'AviTags™', which allow anchoring to SA microspheres via the C-terminus of the protein. When bound to SA microspheres in this configuration, proteins can be displayed in a more uniform orientation that replicates those of the ectodomains of transmembrane proteins or viral spike proteins without destroying potential epitopes. In this study, we coupled a serologically relevant protein antigen, the receptor binding domain (RBD) of severe acute respiratory syndrome coronavirus 2 (SARS-CoV-2) spike protein, to COOH microspheres using conventional cross-linking chemistry and bound an AviTag version of the same antigen to SA microspheres to determine which approach is the most useful when developing microsphere-based serology assays.

MATERIALS AND METHODS

Streptavidin microspheres and biotinylated proteins

Streptavidin microspheres

Latex microspheres functionalized with surface SA were purchased from Bangs Laboratories, which offers them in several different sizes. For this study, 5-micron SA microspheres (Cat. #10010-023) were appropriate for flow cytometry due to their combination of surface area and size. SA is tetrameric but SA-functionalized microspheres are reported by the manufacturer to display an average of two biotin binding sites per SA molecule (**Fig. 1A**). The biotin-binding capacity of SA microspheres is lot-specific and is reported by the manufacturer as the maximal amount of biotin-FITC bound by 1 mg SA microspheres. Biotin-FITC binding capacity values were used to calculate the concentration of AviTag protein needed for surface saturation (lot specific, listed below). For example, 1 mg SA microspheres with a binding capacity of 0.056 µg biotin-FITC (831 Daltons) can bind approximately 2.4 µg of a 35.5 kDa protein, at a 1:1 molar ratio. We loaded SA microspheres at 1:1, ~4:1, and ~10:1 (2.4, 9.6 and 37 µg antigen per mg of SA microspheres, respectively) to ensure complete microsphere saturation.
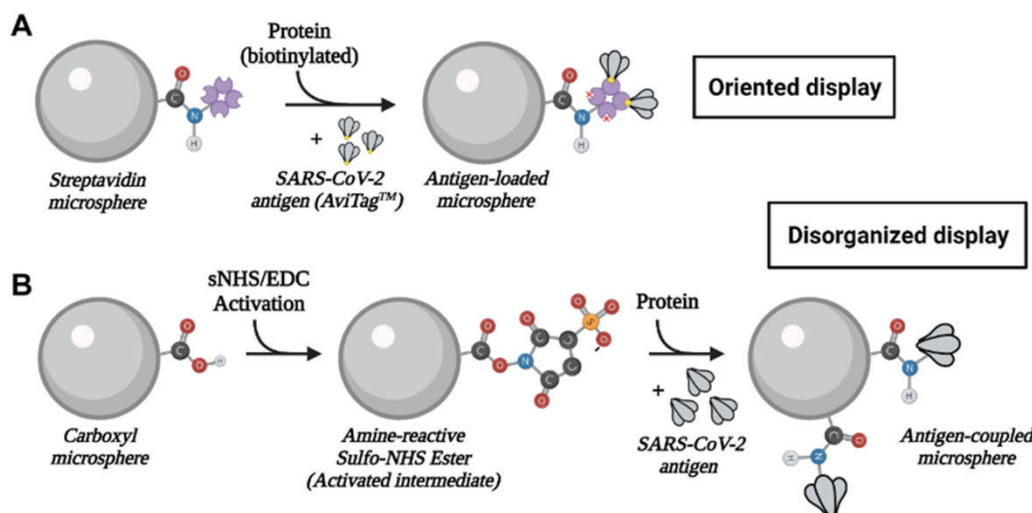

Figure 1 Schematic of microsphere methodologies. A. Streptavidin (SA) microsphere preparation. Proteins with a single biotin at their C-terminus were added directly to SA microspheres forming high affinity biotin:streptavidin interactions between the antigen and the surface of the microsphere that were predicted to result in uniform antigen orientation. SA is depicted as a tetramer (light purple) with an average of two binding sites available for biotin. AviTag™ denotes a BirA biotinylation motif added near the C-terminus of a recombinant protein, which becomes mono-biotinylated in cells engineered to express the BirA biotin ligase. **B.** Carboxyl (COOH) microsphere preparation. COOH microspheres are activated by N-hydroxysulfosuccinimide (sulfo-NHS) and carbodiimide (EDC) creating an amine-reactive sulfo-NHS ester intermediate. Cross-linking to amino acid residues with free amines (e.g. lysine, arginine, asparagine, and glutamine) was predicted to result in disorganized antigen display, which could affect epitope availability.

Biotinylated antigens

Recombinant proteins corresponding to SARS-CoV-2 RBD, nucleocapsid (not present in coronavirus disease (COVID) mRNA vaccines), or a Zika virus protein (non-structural protein 1, NS1) as a negative control, were expressed by the manufacturer in human embryonic kidney cells with a His hexamer for purification and a C-terminal AviTag at the C-terminus for oriented loading. ACROBiosystems (Newark, DE) proteins purchased as mono-biotinylated antigens (Avi-tagged) were: wild-type (Wuhan) SARS-CoV-2 S protein RBD (Cat #SPD-C82E9), SARS-CoV-2 Spike delta variant RBD (L452R, T478K) (Cat #SPD-C82Ed), wild-type SARS-CoV-2 nucleocapsid protein (Cat #NUN-C81Q6), and Zika virus NS1 Protein (Cat #NS1-Z82E9).

Calculation of mono-biotinylated protein binding capacity:

Moles from grams: $\dfrac{binding\ capacity\ of\ spheres\ (as\ \mu g\ biotin - FITC)}{831\ Da\ (MW\ of\ \text{biotin-FITC})}$

Grams from moles: $(moles\ of\ \text{biotin-FITC})\ x\ (formula\ weight\ (Da),\ \text{protein of interest})$

Loading SA microspheres with mono-biotinylated proteins

One milligram (1.43×10^7) of SA microspheres (Bangs Laboratories CP01006, 4.95 μm in diameter, binding capacity 0.056 μg [lot 15284], 0.04 μg [lot 15462], 0.087 μg [lot 15597] biotin-FITC) were washed in phosphate-buffered saline (PBS, Gibco™, Cat #10010-023) by centrifuging them in 12 × 75 mm polypropylene flow tubes (Falcon®, Cat #352063) at 3,000 RCF for 5 minutes at room temperature, then decanting by pipetting. Microspheres were fully resuspended in PBS by pipetting, then loaded with 2.4 μg (1:1, 6 μL), 9.6 μg (~4:1, 24 μL), or 37 μg (~10:1, 92.5 μL) of biotinylated recombinant SARS-CoV-2 RBD (Wuhan) or delta RBD (B.1.617.2) (stock concentration 200 μg/mL) and incubated for 1 hour at room temperature with gentle end-over-end rotation. Control microspheres were prepared identically using 9.6 μg of SARS-CoV-2 nucleocapsid or Zika Virus NS1 antigens, per 1 mg of SA microspheres.

After incubation to load protein, microspheres were washed twice in PBS, 0.05% Tween-20 (hereafter PBS-T) by centrifugation at 3,000 RCF for 5 minutes then decanted. Antigen-coated microspheres were resuspended in 1 mL of UltraBlock-FISH™ Blocking Buffer (Leinco Technologies Inc., Cat #B396), 0.01% Tween-20 (hereafter UBF-T) and stored at 4°C until use.

Carboxyl microsphere methodology

COOH microspheres were covalently bound to free amines of lysine, arginine, asparagine, and glutamine residues present on the antigen proteins in two steps: i) activation (conversion of carboxyl to a stable amine reactive N-hydroxysulfosuccinimide (sulfo-NHS) ester intermediate) and ii) coupling (incubation with recombinant protein during which free amines form amide bonds to the microspheres) (**Fig. 1B**). The antigen used for COOH microsphere coupling was recombinant wild-type SARS-CoV-2 S protein RBD (ACROBiosystems, Cat #SPD-C52H3) with a His tag (no AviTag™).

Activation

One milligram (1.96×10^7) of COOH microspheres (Bangs Laboratories, PCN05005, 4.46 μm in diameter, 10.1% solids, surface charge 11.1 μeq/g) were washed in MES buffer (50 mM MES free acid, pH 6.1) by centrifugation at 3,000 RCF for 5 minutes at room temperature in 12 × 75 mm polypropylene flow tubes, then decanted. Microspheres were fully resuspended in 66.7 μL 50 mM MES buffer by pipetting and held at room temperature while preparing working stocks of Sulfo-NHS chemical modification reagent (Thermofisher, Cat #A39269) and 1-Ethyl-3-(3-dimethylaminopropyl)carbodiimide (EDC) crosslinker (Thermofisher, Cat #A35391).

NOTE: Because Sulfo-NHS and EDC are highly susceptible to hydrolysis we stored them desiccated at 4°C and -20°C, respectively, in aliquots to avoid cycles of warming, hydrating upon exposure to room air, and re-capping. Individual aliquots were always brought to room temperature before opening tubes and adding buffer. These suspensions were always used within minutes, as previously recommended [6].

Working stocks containing 2 mg of sulfo-NHS (1.11 μmol, MW 217.1 g/mol) and 1 mg EDC (1.11 μmol, MW 191.7 g/mol) were prepared separately in 100 μL MES buffer (50 mM). Volumes corresponding to 241 μg sulfo-NHS (12 μL) and 212.8 μg EDC (21.3 μL) of each working stock was added directly to the microspheres in that order and vortexed (in 4-5 pulses, max speed). These amounts of sulfo-NHS and EDC were calculated to be 100 times the total number of COOH on the microspheres (in this case 11.1 nmol per 1 mg), based on the manufacturer's lot-specific measurement of surface charge (*e.g.* 11.1 μeq/g). The mixture was incubated for 20 minutes at room temperature with gentle end-over-end rotation. The activated microspheres were then washed twice in 50 mM MES by centrifugation at 3,000 RCF for 5 minutes, decanted, and resuspended in 100 μL PBS in 12 × 75 mm polypropylene flow tubes. Because activation creates semi-stable intermediates (amine-reactive sulfo-NHS esters, **Fig. 1B**), activated microspheres were always used immediately for coupling, as described below.

Coupling COOH microspheres

The amount of protein antigen used for COOH coupling reactions is calculated as:

$S = (\dfrac{6}{\rho Sd})(C)$, where S is mg protein/g microspheres needed to achieve surface saturation. The input variables are **d**, mean diameter (μm); **ρS**, (μeq COOH per g microspheres) × (gram/mL microspheres); and **C**, capacity of the microsphere surface for a given protein (based on empirically determined values for bovine serum albumin and bovine IgG of 3 mg/m² and 2.5 mg/m², respectively [9]). For our comparison study we chose to use the amount of protein as for SA preparations, which corresponded to 0.65 (2.4 μg), 2.6 (9.6 μg) and 10 (37 μg) times the value of S when calculated for recombinant RBD, respectively.

Coupling to RBD antigen

Prior to activation, selected concentrations of antigen pre-mixes were prepared in order to add them to COOH microspheres immediately after activation and washing them, as described above. Tubes containing 100 µL activated COOH microspheres were resuspended by pulse vortexing, then loaded to the desired concentration with recombinant wild-type SARS-CoV-2 RBD (Wuhan), at a stock concentration of 600 µg/mL, and incubated for 1.5 hours with gentle end-over-end rotation at room temperature. Antigen or antibody coupled microspheres were resuspended by pulse vortexing, then centrifuged at 3,000 RCF for 5 minutes in PBS-T and decanted. Protein-coupled microspheres were resuspended in 1 mL UBF-T and stored at 4°C until use.

> **NOTE:** Prolonged storage of protein coupled COOH microspheres may cause clumping. Pulse sonication (Fisher scientific, Cat #FB50110) at 20 kHz reverses clumping but if the probe tip creates too much heat the microspheres may clump irreversibly.

Coupling to human Immunoglobulin

COOH microspheres were also coupled to human immunoglobulin (Ig) representing all possible isotypes for use as controls to evaluate the specificity of fluorescent 'detector' monoclonal antibodies (mAbs). The Ig were isolated from plasma of healthy donors or myeloma patients by the manufacturer, Athens Research & Technology (Athens, GA). For each 1 mg ($1.96 × 10^7$) freshly activated microspheres 37 µg of human Ig was added and processed as described for RBD coupling above.

Human immunoglobulins used in this study were IgD (Cat #16-16-090704-M), IgA1 (Cat #16-16-090701-1M), IgA2 (Cat #16-16-090701-2M), IgE (Cat #16-16-090705), IgG1 (Cat #16-16-090707-1), IgG2 (Cat #16-16-090707-2), IgG3 (Cat #16-16-090707-3), IgG4 (Cat #6-16-090707-4), and IgM (Cat #16-16-090713).

Tests of RBD loading and epitope availability

RBD antigen coupling to COOH or SA microspheres was confirmed by flow cytometric staining with various RBD-specific human monoclonal antibodies (ACROBiosystems, Newark, DE). All but one of these antibodies were cloned from COVID-19 patients and recombinantly expressed in HEK293 by the manufacturer. The antibody products were ACROBiosystems recombinant anti-SARS-CoV-2 Spike RBD Neutralizing Antibody, Human IgG1 (AS35) (Cat #SAD-S35), Human IgG1 (AM180) (Cat #SPD-M180), Human IgM (AM122) (Cat #SPD-M162). One of the RBD-specific antibodies, was expressed as a chimeric Human IgM (AM130) (Cat #SPD-M141), combining the constant domains of human IgM with mouse variable regions of an RBD-specific mAb.

Flow cytometry was performed by resuspending $4 × 10^4$ RBD-coupled microspheres per stain in 100 µL UBF-T in each well of a 96-well microtiter plate (V-bottom, costar®, Cat # 3897),

then centrifuged at 3,000 RCF for 5 minutes and decanting by pipetting. Microspheres were resuspended in UBF-T containing primary antibody diluted to the desired concentration in 100 µL and incubated for 30 minutes at room temperature with gentle plate shaking (150 RPM, Fisherbrand™ Microplate Shaker, model #88881023). Microspheres were then washed twice by adding 100 µL PBS-T, centrifuged at 3,000 RCF for 5 minutes, then decanted. Microspheres were resuspended in 100 µL UBF-T containing anti-human Ig-detector monoclonal antibodies and incubated for 30 minutes at room temperature in the dark. After incubation, the microspheres were centrifuged at 3,000 RCF for 5 minutes, then decanted. Finally, the stained microspheres were washed twice in 100 µL PBS-T and fully resuspended in 200 µL PBS and placed in 12 × 75 mm polypropylene flow tubes.

Serum samples

Venous blood was drawn from healthy individuals using standard phlebotomy techniques with approval of the UofL Institutional Review Board, IRB number 14.0661. Consented donors, recently immunized with Pfizer/BioNTech COVID vaccine BNT162b2 as part of a campus-wide vaccination drive, volunteered to provide 4–5 mL peripheral blood at various times following immunization through 240 days (8 months). Blood samples were collected from all individuals (N = 5) into BD Vacutainer SST serum separation tubes (BD Biosciences, Cat #368013), inverted, then incubated at room temperature for 30 minutes prior to centrifugation at 1200 × g for 10 minutes (room temperature). The sera were transferred to fresh tubes and centrifuged again to remove residual red blood cells. Coded serum samples were aliquoted, 0.2 mL per 1.5 mL Eppendorf tubes (Eppendorf®, 0.5 mL, Cat #022363611), and stored at -80°C until use.

Detector antibodies

Isotype-specific secondary, or 'detector' antibodies, were used to measure RBD-specific antibody titers in the immunized individuals. The detector antibodies used (SouthernBiotech, Birmigham, AL) were: mouse anti-human IgM-Alexa Fluor® 647 (SA-DA-4, Cat #9020-31), mouse anti-human IgD-Alexa Fluor® 647 (IADB6, Cat #9030-31), mouse anti-human IgG1 hinge-Alexa Fluor® 647 (4E3, Cat #9052-31), mouse anti-human IgG2 Fc-PE (31-7-4, Cat #9060-09), mouse anti-human IgA1-Alexa Fluor® 647 (B3506B4, Cat #9130-31), mouse anti-human IgA2-Alexa Fluor® 647 (A9604D2, cat no. 9140-31), mouse anti-human IgE Fc-Alexa Fluor® 647 (B3102E8, Cat #9160-31), mouse anti-human IgG4 Fc-Alexa Fluor® 647 (HP6025, Cat #9200-31), mouse anti-human IgG3 Hinge-Alexa Fluor® 647 (HP6050, Cat #9210-31).

Flow cytometric serology

To detect antigen-specific antibodies in sera from vaccinated

blood donors, RBD-coated SA microspheres were plated (4×10^4/well) in 96-well V-bottom plates and centrifuged at 3,000 RCF for 5 minutes then decanted. Diluted serum (1:300 in UBF-T) was added to the microspheres and mixed by gentle pipetting, then incubated for 30 minutes with plate shaking (150 RPM). After incubation, the plate was centrifuged at 3,000 RCF for 5 minutes then decanted. The plate was washed twice in PBS-T, decanted, and resuspended in 100 µL UBF-T containing 'detector' mAbs diluted to the desired concentration and incubated for 30 minutes at room temperature in the dark without agitation. After incubation, the microspheres were centrifuged at 3,000 RCF for 5 minutes then decanted. Stained microspheres were washed twice in 100 µL PBS-T then decanted. Finally, the stained microspheres were resuspended in 200 µL PBS then transferred to polypropylene 12 × 75 mm polypropylene flow tubes for flow cytometry.

A 3-laser Cytek™ Northern Lights NL-3000 flow cytometer, operated with SpectroFlo software (v2.2.0.3) was used for the visualization of stained microspheres (~5,000 events). The gating scheme (**Fig. S1**) was as follows: visible light was used to gate on singlets (FSC-A × SSC-A) as shown. This gate was confirmed to contain singlets by viewing as FSC-A x FSC-H and SSC-A x SSC-H plots (not shown). Histograms were generated by plotting the peak florescence (channel R2 for Alexa Fluor 647 and B4 for PE) against microsphere count (y-axis).

Flow cytometric analysis, including figure generation, was performed with FlowJo (v10.8.0) software. Separation index calculations were performed using a formula, below, described in "FlowJo for Antibody Titrations: Separation Index and Concatenation" [10]. Additional gating was performed for these calculations, such as negative gates as determined from unstained controls.

$$\text{Separation index: } \frac{median \, (positive) - median \, (negative)}{\left(\frac{84th \, percentile \, (median \, background) - median \, (negative)}{0.995}\right)}$$

In brief, the 'table editor' function in FlowJo was used to input values (*e.g.* median) from the experimental flow plots. The formula above was typed in the 'formula' tab, then applied to the defined data set generating a table of separation index values.

RESULTS AND DISCUSSION

Antigen loading on COOH versus SA microspheres

The goal of this study was to develop a serological assay method that does not depend on enzyme-linked immunosorbent assay (ELISA), which can require large amounts of recombinant antigen relative to microsphere-based cytometry. Our initial efforts with COOH microspheres highlighted challenges with use of the COOH cross-linking chemistry such that we investigated, and report here, a method that does not require expertise with chemical cross-linking chemistries. We compare an optimized COOH crosslinking protocol to an alternative approach in which commercially available, mono-biotinylated antigens can be simply mixed with SA-functionalized microspheres.

To do this, SARS-CoV-2 RBD protein was bound to COOH and SA microspheres at ~1:1, ~4:1, or ~10:1 ratios of protein:microspheres, then stained with RBD-specific mAb. The extent of protein loading was then measured by flow cytometry (**Fig. 2**). We found significant differences in staining, however, the signal was robust for both microsphere types (**Fig. 2A**). RBD-coupled COOH microspheres produced less signal at the highest protein:microsphere ratio, suggesting that COOH microspheres may be more prone to 'over-saturation' compared to SA microspheres which more consistently reached a stable plateau (**Fig. 2 and data not shown**). Although the exact reason for the decreased signal is unclear, we hypothesized that the cross-linking chemistry used to generate COOH microspheres is more likely to lead to multiple layers of protein in a manner that prevents the mAb from binding to its epitope. This effect is not expected with mono-biotinylated antigens bound to SA microspheres due to the finite number of binding interactions that are possible.

Epitope accessibility

The apparent over-saturation effect observed with COOH microsphere coupling (**Fig. 2A**) at the highest protein:microsphere ratio suggested that, under some conditions, epitope accessibility can be limited by disoriented antigen display. To investigate in greater detail whether antigen orientation could contribute to differences in staining due to antibody epitope accessibility, we stained COOH and SA microspheres with different clones of RBD-specific mAb, each recognizing a different surface epitope. Initially, it appeared antibody binding was lower with SA compared to COOH microspheres for both mAbs tested (**Fig. 2B**), depending on the lot of SA microspheres used. Further investigation showed that this inconsistent staining correlated with different lots that were rated by the manufacturer as having different binding capacities, as measured by the amounts of biotin-FITC needed to reach saturation (**Fig. 2B & 2C**).

Fluorescence intensity is determined by antigen abundance such that lower binding capacity would be expected to reduce staining signal. To test this, we obtained a third microsphere lot (15597) with a different binding capacity than the previous two lots (**Fig. 2C**) and observed differences in RBD staining signal in proportion to the measured binding capacity for biotin-FITC. Overall, we concluded that epitope accessibility of COOH was not less than that of SA microspheres, provided the COOH cross-linking step was not performed with excessive amounts of protein antigen. In addition, fluorescence intensity of stains for antigen on SA microspheres was consistently predicted by binding capacity for biotin-FITC.

Overall, our comparison of COOH and SA microspheres indicated they have similar staining profiles and antigen epitope accessibility. COOH microspheres seemed more prone to protein over-saturation, such that protein:microsphere ratios need to be more stringently tested to optimize antigen loading. Due to the ease and consistency of loading mono-biotinylated (AviTag)

proteins on SA microspheres, we decided to test this approach more extensively in a small human serology study.
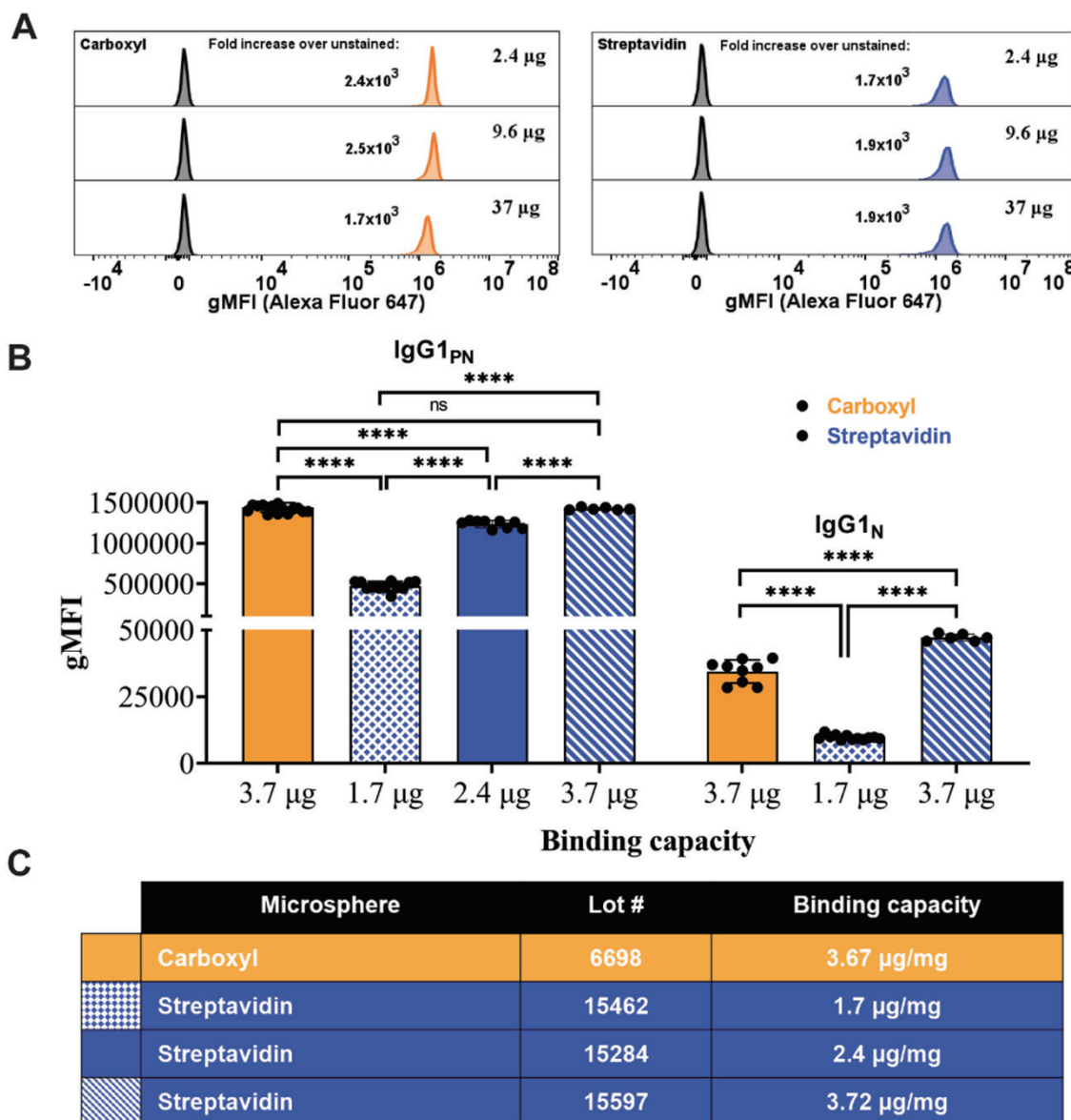

Figure 2 Antigen staining is robust for carboxyl and streptavidin microspheres. Carboxyl (COOH) and Streptavidin (SA) microspheres were bound to recombinant severe accurate respiratory syndrome coronavirus 2 (SARS-CoV-2) receptor binding domain (RBD) protein then stained with various primary and secondary monoclonal antibodies (mAbs) for flow cytometry. A. COOH (orange) and SA microspheres (blue) stained with RBD-specific IgG1. Shown are measurements of geometric mean fluorescence intensity (gMFI) as flow cytometric histograms, after loading microspheres with the indicated amounts of RBD (see methods for molar ratios and staining with $IgG1_{PN}$ mAb) Negative histogram peaks show background signal from unstained RBD microspheres. **B.** RBD bound COOH and SA microspheres were stained with RBD-specific IgG1 each recognizing different RBD epitopes. Shown are measurements of antibody binding (bar graphs) after staining with the indicated mAb clones. The bars represent the average of technical triplicates of N=3, error bars indicate S.D.P values represent a comparison between COOH and each lot of SA for each antibody clone using an ordinary one-way ANOVA. **C.** Table indicating the different lots and surface saturation values of the microspheres used in this experiment.

Cross-reactivity of detector human Ig antibodies

We next evaluated the performance of SA microspheres in a serological assay for antigen-specific antibodies generated in response to BioNTech/Pfizer COVID mRNA vaccination. Vaccine clinical trials generally assess humoral responses by measuring vaccine antigen-specific IgG, without distinguishing amongst the four IgG subtypes, 1–4, despite having their markedly different roles in humoral responses. Because we are interested in more precise assays of humoral responses, we sought to use RBD loaded SA microspheres to distinguish between IgG subtypes. To do this, it was first necessary to determine the level of cross-reactivity

for IgG subtype-specific 'detector' mAbs.

To evaluate the extent to which commercially available anti-human Ig mAbs were cross-reactive, we generated a stain matrix by coupling individual human immunoglobulins directly to COOH microspheres and staining them with each detector antibody. As expected, all detector antibodies produced specific signal (**Fig. 3**). We also found that most detector antibodies were cross-reactive to varying degrees when tested for staining of microspheres loaded with un-related Ig isotypes, with the most promiscuous antibody being anti-IgG2 mAb clone (31-7-4). Anti-IgG1 gave robust signal for its intended target, with some cross-reactivity for IgG3 and IgG2. However, the IgG1-specific signal was markedly higher than the cross-reactivity for IgG2 and IgG3. Anti-IgA1 was similarly cross-reactive with IgG3, and also IgM, although the specific signal was ~10 times higher than the non-specific signal. Overall, these findings revealed that detector mAbs are cross-reactive for irrelevant isotypes immobilized on microspheres, which was not observed by the manufacturer in its quality control testing of the same detectors for use in microplate-based ELISA or fluorescent-linked immunosorbent assay (FLISA).
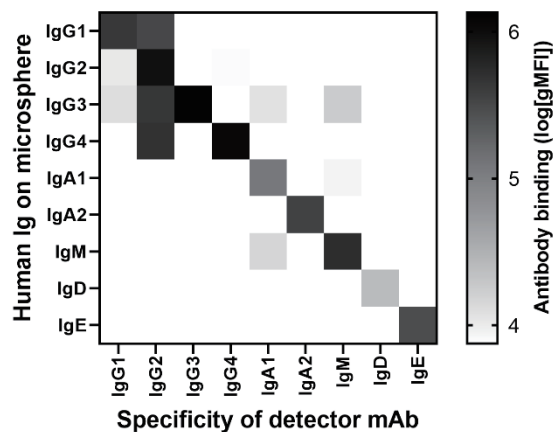

Figure 3 Detector antibody cross-reactivity is present and variable between detectors. Purified human Ig representing all isotypes coupled to carboxyl (COOH) microspheres were used to evaluate cross-reactivity of isotype-specific detector monoclonal antibodies (mAbs). Shown is a staining matrix in which each detector antibody was tested for binding to the indicated human immunoglobulin (Ig). Binding of detector mAbs is depicted on a log scale, where the darker shading indicates larger values (max, 2×10^6 gMFI). Background was set at 7500 gMFI, corresponding to the average intensity of unstained microspheres.

Detector cross-reactivity between IgG subtypes is concentration-dependent

To determine if IgG subtype cross-reactivity could be minimized by changing concentration of the fluorescently labelled detector mAbs, we tested some of the isotype-specific detectors on mixtures of Ig-coated microspheres. First, we mixed IgG3-with IgG1-coupled microspheres 1:1 (**Fig. 4A**) and stained with a range of anti-IgG1 mAb concentrations (0.03–2 μg/mL). Flow cytometry was then performed to determine the mAb concentration at which specific signal was robust with minimal cross-reactivity. Separation index values were calculated as the distance between positive and negative peaks, with a correction for negative peak 'spread' (**Fig. 4B**). As expected, cross-reactivity was detector concentration dependent, with the highest separation index values at lower detector concentrations (0.03 and 0.06 μg/mL) and lower separation index values at higher concentrations (1 and 2 μg/mL) (**Fig. 4C**). Because the highest separation index value for a mixture of IgG1 and IgG3 was achieved with 0.06 μg/mL anti-IgG1, this mAb concentration was chosen for measurement of vaccine-antigen specific IgG1. Because a previous study that showed Pfizer BNT162b2 mRNA vaccine recipients (N=24) produced antigen-specific IgG1, IgG3, and IgA1 [4], we also determined cross-reactive separation index values for IgG3- and IgA1-specific detector mAbs (data not shown).

IgG1, IgG3, and IgA1 specific for Wild-type and Delta variant RBD are detectable in BioNTech/Pfizer BNT162b2 vaccine recipients

To evaluate IgG1, IgG3, and IgA1 humoral responses to immunization, we collected sera from five participants various times after immunization with BNT162b2. Sampling times including prior to or the day of vaccine Dose 1, then days 7, 14, and 21 afterward (prior to Dose 2). Sera collection continued 9 days after Dose 2 (Day 30), then at 1–2 month intervals thereafter.

After pilot experiments confirmed the peak antibody response to immunization occurred on Day 30, aliquots of sera collected at this timepoint were used to determine the appropriate dilution of sera to use; 1:300 was found to be optimal with respect to maximizing positive signal with the least background 'noise' from blank SA microspheres. In addition to SA-microspheres loaded with RBD antigen, we also tested responses to Zika Virus NS1 (ZV NS1) and SARS-CoV-2 Nucleocapsid protein (which is not encoded by the mRNA vaccines) to SA microspheres to evaluate antibody specificity and immune status prior to immunization, respectively. Finally, we coupled SARS-CoV-2 variant RBD (B.1.617.2) to SA microspheres to compare antibody binding to wild-type or RBD of a variant (delta) that was in circulation at the time these samples were collected.

IgG1, the most abundant antibody in serum, was the first target for assay evaluation. All participants (CV1-5) began producing RBD-specific IgG1 by Day 14 after Dose 1. None appeared to have been previously exposed to SARS-CoV-2 prior to Dose 1, as indicated by the lack of RBD-specific signal, relative to control antigen ZV NS1 (**Fig. 5A, B; D0 and D7**). The conclusion that none of the study participants had been infected by SARS-CoV-2 prior to immunization was further supported by the absence of antibody responses to SARS-CoV-2 nucleocapsid (**Fig. 5B**).
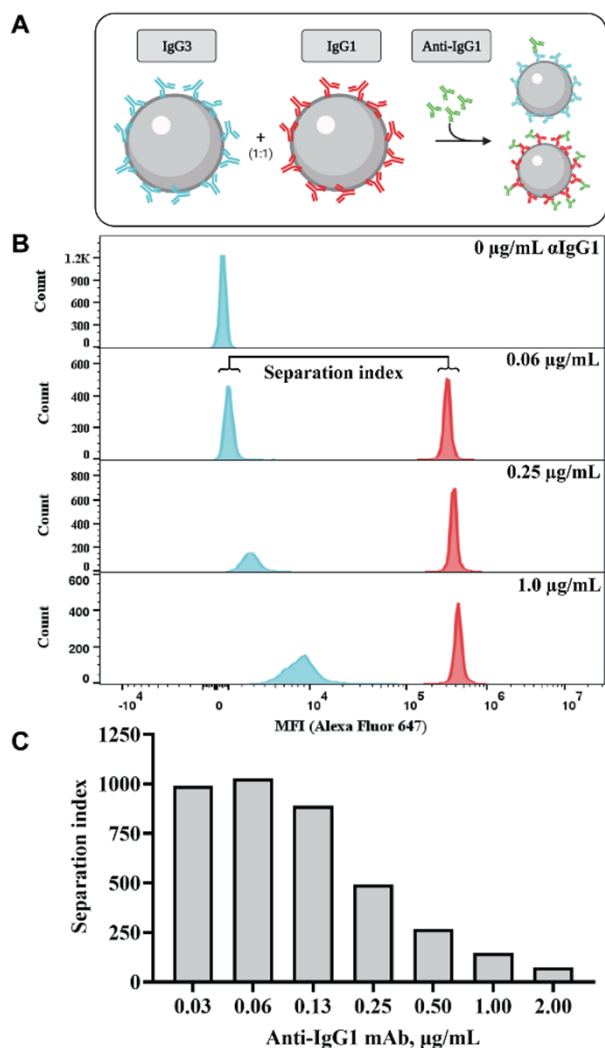
Figure 4 Detector mAb cross-reactivity between IgG subtypes is concentration-dependent. A. IgG1 and IgG3 coupled microspheres were mixed in a 1:1 ratio, then stained with anti-IgG1. Shown are **B.** Representative histograms of flow cytometric signal from IgG3 (blue) or IgG1 (red) microspheres after staining with the indicated amounts of anti-IgG1 detector mAb. **C.** Separation index values at specified concentrations. See Methods for the separation index formula.

Tests of subsequent times points allowed us to assess durability of the IgG1-associated vaccine response (**Fig. 5A, B**). Of note, we found that the magnitudes of the peak antibody responses on Day 30 for each participant, were not consistently predictive of later titers. For example, sera from study participants CV3 and CV4 had similar peak titers on Day 30 which had diverged by the end of 240 days, while CV2 and CV1 showed somewhat different peak titers which had converged by Day 120 and remained indistinguishable through Day 240 (**Fig. 5A**). Additional tests with SA-microspheres loaded with mono-biotinylated RBD corresponding to that of the Delta variant were performed to investigate antibody binding differences between wild-type and variant antigen. As shown in **Figure 5**C and **D**, antibodies

produced against wild-type (WT) and Delta variant RBD were broadly similar through Day 240 with significant differences at peak titer (Day 30) for three donors.

IgG3-associated vaccine responses were tested next to show that the SA microspheres coated with RBD can be used to detect different IgG subtypes. We found that all individuals produced RBD-specific IgG3, with a time-to-peak response that was similar to that of IgG1 (**Fig. 6A, upper panel**). However, inter-individual variability was greater in terms of magnitude for Day 30 peak IgG3 responses than for IgG1. The IgG3 responses of all individuals returned to baseline levels by 240 days (**Fig. 6A**) and, as with IgG1, IgG3 binding to WT and Delta variant RBD was most noticeably different at peak titer (Day 30) (**Fig. 6A, lower panel**).

Lastly, we tested IgA-associated responses. All study individuals produced vaccine antigen-specific IgA1 after immunization that, like IgG3, seemed to be more variable amongst the study participants (**Fig. 6B**). Interestingly, for participants CV1 and CV3-5, there was a bimodal response indicated by a decrease in titers between Dose 1 and Dose 2 (**Fig. 6B**). Serum IgA1 positivity was even more short-lived than IgG3 in returning to baseline by Day 30, consistent with the short half-life of human IgA1 in serum [11, 12]. This finding was similar to that of another study, in which IgA responses after COVID vaccination were only slightly above baseline by 3 weeks post-vaccination [4]. Finally, IgA1 binding to WT and Delta variant RBD were broadly similar like IgG1 and IgG3 with donor variability in responses primarily at peak titer (Day 30) (**Fig. 6B**).

Overall, IgG1, IgG3, and IgA1 responses could be detected in BioNTech/Pfizer BNT162b2 vaccinated participant sera using SA microspheres loaded with mono-biotinylated protein, with sufficient sensitivity to detect inter-individual variability amongst the five participants in our small study. Detection of these antibodies was highly antigen-specific, as shown by the lack of signal for ZV NS1 and SARS-CoV-2 nucleocapsid loaded microspheres. Hence, SA microspheres can be readily loaded with mono-biotinylated recombinant antigens for use in bead-based flow serological assays and thus provides an alternative approach for antibody detection in post-vaccination serum.

Our interest in comparing wild-type (Wuhan) to Delta variant RBD was due to early reports showing an increase in breakthrough cases with Delta SARS-CoV-2 in fully vaccinated individuals [13]. Because fully vaccinated individuals are reported to have lower neutralizing antibody titers for the Delta variant [14, 15], we expected to be able to detect differences in antibody binding or rate of decay, or both, between delta variant RBD and wild-type (Wuhan). However, antibody binding to WT and Delta variant RBD was largely similar across all five study participants for all Ig isotypes tested, IgG1, IgG3, and IgA1 through 240 days. Delta variant RBD contains only two mutations compared to Wuhan [16]. Moreover, it appears that vaccine recipients differentially produce neutralizing antibodies against RBD, the N-terminal domain (NTD) of S1 and Spike, with the lowest percentage against

RBD [17]. Therefore, antibody binding similarities between Delta variant and WT (Wuhan) RBD in vaccinated individuals is, in retrospect, not surprising given minimal mutational differences and a lower proportion of neutralizing antibodies specific for RBD.
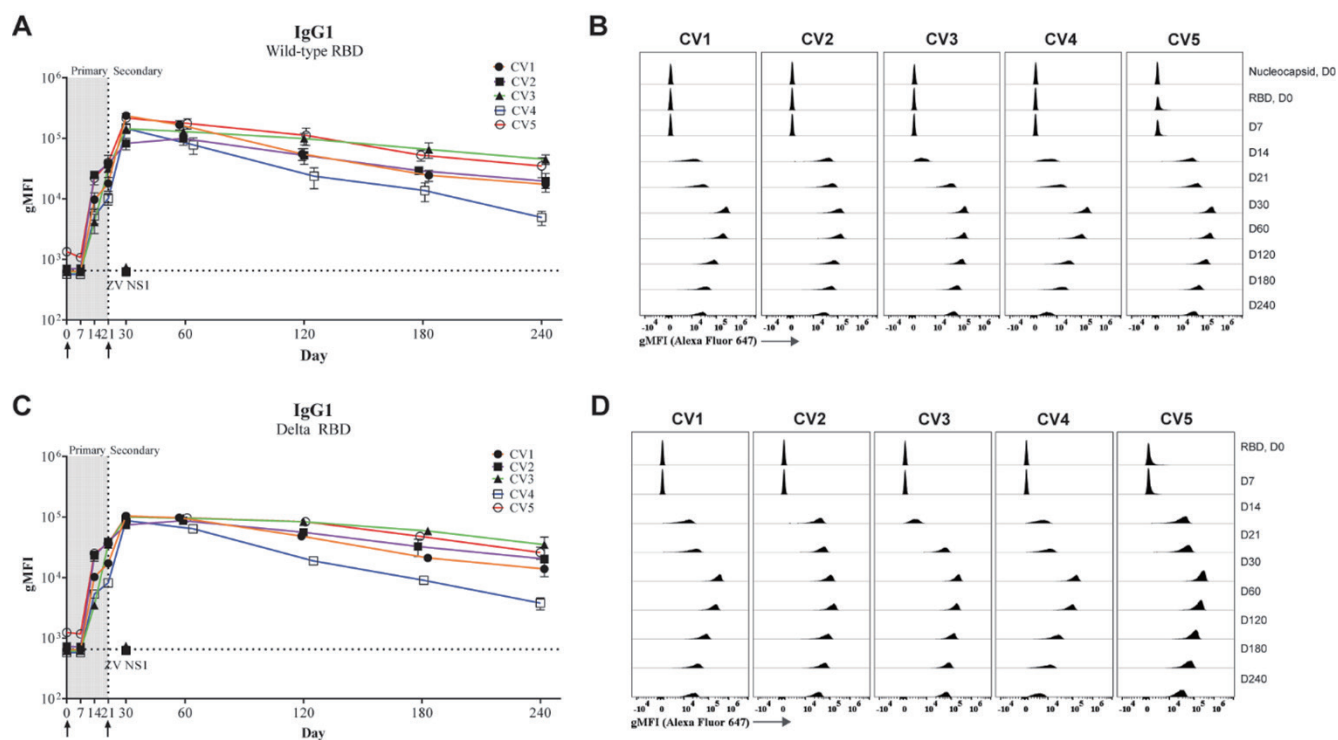

Figure 5 SARS-CoV-2 RBD-specific IgG1 after vaccination with BioNTech/Pfizer COVID-19 vaccine BNT162b2. Streptavidin (SA) microspheres were loaded with wild-type (Wuhan) or delta variant receptor binding domain (RBD) antigen, incubated with serum from immunized individuals, and then stained with human IgG1-specific detector monoclonal antibody (mAb) (0.06 µg/mL). Shown is IgG1 signal over 240 days for each individual's response to RBD from (**A, B**) wild-type RBD (Wuhan) or (**C, D**) delta variant SARS-CoV-2. (**A, C**) Microspheres loaded with irrelevant antigen, Zika Virus NS1 (ZV NS1), were incubated with Day 30 post-vaccination serum as a specificity control. The lower limit of detection (dotted line) was determined as the average signal (N=5) after staining RBD microspheres with pre-immune sera. Results shown are averages from (**A, B**) N=3 and (**C, D**) N=2 independent experiments; error bars indicated S.D.

Protective immunity was not assessed in this study, beyond that indicated by generation of vaccine antigen-specific humoral responses. However, general conclusions can be made about correlates of protection based on previously reported studies. As measured by fluorescence intensity, IgG1 signal on Day 180 (6 months) had fallen to 21% of peak and furthered declined to 14% of peak by Day 240 (8 months). Our time course shows that the loss of antibody signal after peak occurs at a steady rate for each participant, suggesting that protective immunity would wane at a similarly steady rate. The Pfizer BNT162b2 vaccine clinical trial data shows protection against COVID-19 is 91% seven days after Dose 2 [18] and several reports show immunity wanes significantly by 6 months post-vaccination [19, 20].

CONCLUSIONS

Cross-linking protein antigens to COOH microsphere preparations is a multi-step process with technical challenges. First, activation of COOH groups on the microspheres requires chemical modification and cross-linking reagents, such as sulfo-NHS and EDC, respectively, which are highly sensitive to hydrolysis and buffer pH. Suboptimal pH or storage conditions can reduce or destroy functionality of these reagents. Moreover, the concentrations and molar ratios of sulfo-NHS and EDC are important determinants of high-density cross-linking, causing reduced protein coupling if the concentrations are limiting. The amine-reactive sulfo-NHS ester intermediate produced during activation is semi-stable, however, the stability is markedly reduced under aqueous conditions. Finally, protein coupled carboxyl microspheres seemed more susceptible to clumping than SA microspheres and were difficult to disperse once clumping had occurred in storage.

On the other hand, SA microsphere preparations are simple to make. The absence of any cross-linking reagents in preparation of SA microspheres makes loading them with biotinylated protein more robust because the two components can be simply mixed together, with no observable risk of over-saturation as seemed to occur with COOH microspheres. In our experience, protein loaded streptavidin microspheres were more easily and consistently prepared.
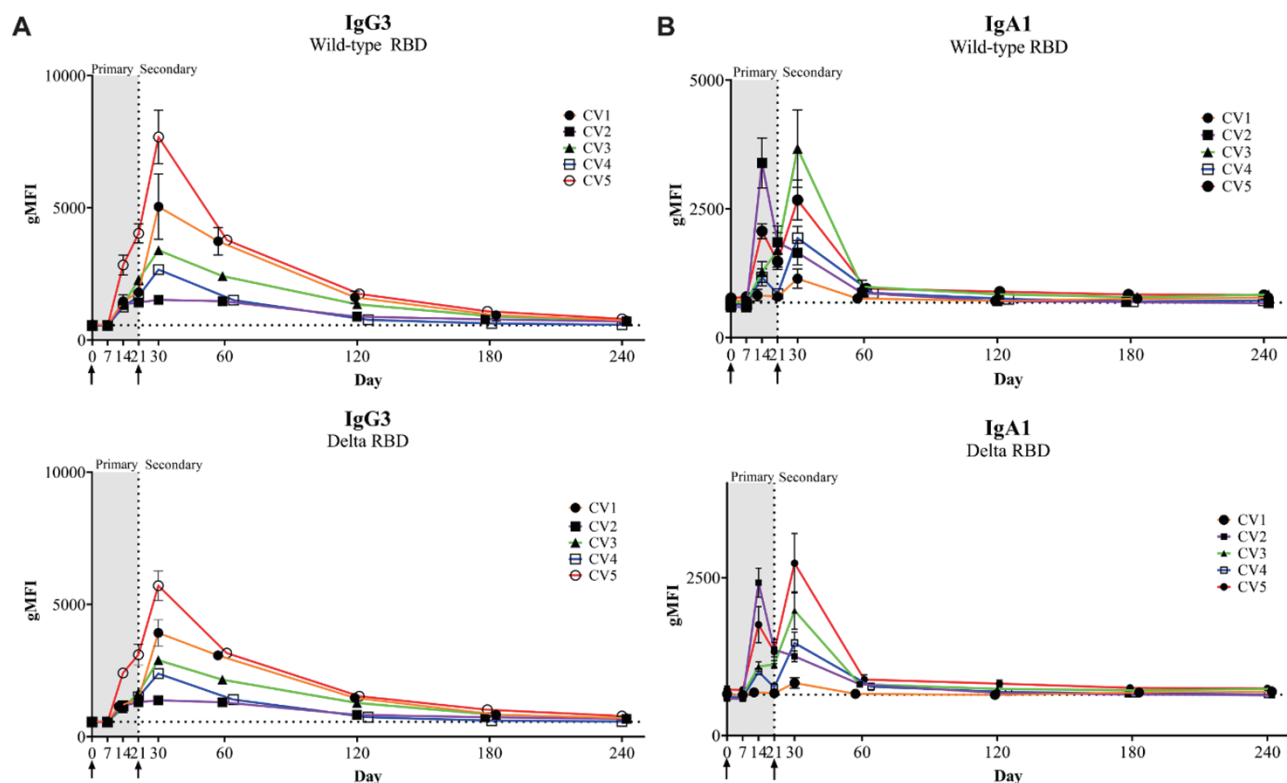
Figure 6 Serologic measurement of antigen-specific IgG3 and IgA1 using SA microspheres. Streptavidin (SA) microspheres were loaded with wild-type (Wuhan) or delta variant receptor binding domain (RBD) antigen, incubated with serum from immunized individuals, then stained with human (A) IgG3- or (B) IgA1-specific detector monoclonal antibodies (mAbs) (0.125 µg/mL for both). The lower limit of detection (dotted line) was determined as the average signal (N=5) from pre-immune sera. Results shown are averages from (A, B) N=3 for wild-type RBD (Wuhan) and (A, B) N=2 for delta variant RBD SA microspheres, error bars indicate S.D.

Here, we made use of the wealth of pandemic-related reagents to evaluate the use of SA microspheres loaded with C-terminally anchored proteins in a flow cytometric serology assay. The increasing use of Avi-Tag technology and mammalian cells to express C-terminally biotinylated proteins, along with an abundance of humanized monoclonal antibodies with specificity for the RBD of SARS-CoV-2 spike protein allowed us to readily measure humoral responses to the BioNTech/Pfizer BNT162b2 COVID vaccine in a small cohort of immunized individuals. Ours was not the first study to report the utility of microspheres loaded with mono-biotinylated antigens; Jantarabenjakul *et al*, for example, used them to devise a clever assay for SARS-CoV-2 neutralizing antibodies [21] whereas we evaluated them in the context of flow cytometric measurement of overall humoral responses to an immunogen. We found that His-AviTag™ RBD protein could be easily and stably loaded onto SA microspheres at an antigen density that directly reflected the number of available biotin-binding sites. Microspheres prepared in this manner were sufficient to detect RBD-specific IgG1, IgG3, and IgA1 in the sera of immunized persons when tested in a time course of their individual humoral responses. These findings show that SA microspheres loaded with mono-biotinylated AviTag™ proteins are an alternative to COOH microspheres for use in flow cytometric

serology, and likely other types of biological assays, in which the orientation of the loaded proteins is relevant.

References

1. Fong CH, Cai JP, Dissanayake TK, Chen LL, Choi CY, Wong LH, et al. Improved Detection of Antibodies against SARS-

CoV-2 by Microsphere-Based Antibody Assay. Int J Mol Sci. 2020 Sep;21(18):E6595. https://doi.org/10.3390/ijms21186595 PMID:32916926

2. Dobaño C, Vidal M, Santano R, Jiménez A, Chi J, Barrios D, et al. Highly Sensitive and Specific Multiplex Antibody Assays To Quantify Immunoglobulins M, A, and G against SARS-CoV-2 Antigens. J Clin Microbiol. 2021 Jan;59(2):e01731-20. https://doi.org/10.1128/JCM.01731-20 PMID:33127841

3. Rogier EW, Moss DM, Mace KE, Chang M, Jean SE, Bullard SM, et al. Use of Bead-Based Serologic Assay to Evaluate Chikungunya Virus Epidemic, Haiti. Emerg Infect Dis. 2018 Jun;24(6):995–1001. https://doi.org/10.3201/eid2406.171447 PMID:29774861

4. Fraley E, LeMaster C, Geanes E, Banerjee D, Khanal S, Grundberg E, et al. Humoral immune responses during SARS-CoV-2 mRNA vaccine administration in seropositive and seronegative individuals. BMC Med. 2021 Jul;19(1):169. https://doi.org/10.1186/s12916-021-02055-9 PMID:34304742

5. Tcherniaeva I, den Hartog G, Berbers G, van der Klis F. The development of a bead-based multiplex immunoassay for the detection of IgG antibodies to CMV and EBV. J Immunol Methods. 2018 Nov;462:1–8. https://doi.org/10.1016/j.jim.2018.07.003 PMID:30056034

6. Bugiel M, Fantana H, Bormuth V, Trushko A, Schiemann F, Howard J, et al. Versatile microsphere attachment of GFP-labeled motors and other tagged proteins with preserved functionality. J Biol Methods. 2015;2(4):e30. https://doi.org/10.14440/jbm.2015.79

7. O'callaghan CA, Byford MF, Wyer JR, Willcox BE, Jakobsen BK, McMichael AJ, et al. BirA enzyme: production and application in the study of membrane receptor-ligand interactions by site-specific biotinylation. Anal Biochem. 1999 Jan;266(1):9–15. https://doi.org/10.1006/abio.1998.2930 PMID:9887208

8. Ioannou M, Papageorgiou DN, Ogryzko V, Strouboulis J. Mammalian expression vectors for metabolic biotinylation tandem affinity tagging by co-expression in cis of a mammalian codon-optimized BirA biotin ligase. BMC Res Notes. 2018 Jun;11(1):390. https://doi.org/10.1186/s13104-018-3500-9 PMID:29898783

9. Cantarero LA, Butler JE, Osborne JW. The adsorptive characteristics of proteins for polystyrene and their significance in solid-phase imunoassays. Anal Biochem. 1980 Jul;105(2):375–82. https://doi.org/10.1016/0003-2697(80)90473-X PMID:7006446

10. FlowJo For Antibody Titrations- Separation Index and Concatenation. Flow Cytometry Core, Carbone Cancer Center, University of Wisconsin. Cited on May 5, 2016. Available from: http://www.uwhealth.org/flowlab.

11. Morell A, Skvaril F, Noseda G, Barandun S. Metabolic properties of human IgA subclasses. Clin Exp Immunol. 1973 Apr;13(4):521–8. PMID:4717094

12. Davis SK, Selva KJ, Kent SJ, Chung AW. Serum IgA Fc effector functions in infectious disease and cancer. Immunol Cell Biol. 2020 Apr;98(4):276–86. https://doi.org/10.1111/imcb.12306 PMID:31785006

13. Christensen PA, Olsen RJ, Long SW, Subedi S, Davis JJ, Hodjat P, et al. Delta Variants of SARS-CoV-2 Cause Significantly Increased Vaccine Breakthrough COVID-19 Cases in Houston, Texas. Am J Pathol. 2022 Feb;192(2):320–31. https://doi.org/10.1016/j.ajpath.2021.10.019 PMID:34774517

14. Davis C, Logan N, Tyson G, Orton R, Harvey WT, Perkins JS, et al.; COVID-19 Genomics UK (COG-UK) Consortium; COVID-19 DeplOyed VaccinE (DOVE) Cohort Study investigators. Reduced neutralisation of the Delta (B.1.617.2) SARS-CoV-2 variant of concern following vaccination. PLoS Pathog. 2021 Dec;17(12):e1010022. https://doi.org/10.1371/journal.ppat.1010022 PMID:34855916

15. Edara VV, Pinsky BA, Suthar MS, Lai L, Davis-Gardner ME, Floyd K, et al. Infection and Vaccine-Induced Neutralizing-Antibody Responses to the SARS-CoV-2 B.1.617 Variants. N Engl J Med. 2021 Aug;385(7):664–6. https://doi.org/10.1056/NEJMc2107799 PMID:34233096

16. Kumar S, Thambiraja TS, Karuppanan K, Subramaniam G. Omicron and Delta variant of SARS-CoV-2: A comparative computational study of spike protein. J Med Virol. 2022 Apr;94(4):1641–9. https://doi.org/10.1002/jmv.27526 PMID:34914115

17. Amanat F, Thapa M, Lei T, Ahmed SM, Adelsberg DC, Carreño JM, et al.; Personalized Virology Initiative. SARS-CoV-2 mRNA vaccination induces functionally diverse antibodies to NTD, RBD, and S2. Cell. 2021 Jul;184(15):3936–3948.e10. https://doi.org/10.1016/j.cell.2021.06.005 PMID:34192529

18. Polack FP, Thomas SJ, Kitchin N, Absalon J, Gurtman A, Lockhart S, et al.; C4591001 Clinical Trial Group. Safety and Efficacy of the BNT162b2 mRNA Covid-19 Vaccine. N Engl J Med. 2020 Dec;383(27):2603–15. https://doi.org/10.1056/NEJMoa2034577 PMID:33301246

19. Levin EG, Lustig Y, Cohen C, Fluss R, Indenbaum V, Amit S, et al. Waning Immune Humoral Response to BNT162b2 Covid-19 Vaccine over 6 Months. N Engl J Med. 2021 Dec;385(24):e84. https://doi.org/10.1056/NEJMoa2114583 PMID:34614326

20. Tartof SY, Slezak JM, Fischer H, Hong V, Ackerson BK, Ranasinghe ON, et al. Effectiveness of mRNA BNT162b2 COVID-19 vaccine up to 6 months in a large integrated health system in the USA: a retrospective cohort study. Lancet. 2021 Oct;398(10309):1407–16. https://doi.org/10.1016/S0140-6736(21)02183-8 PMID:34619098

21. Jantarabenjakul W, Sodsai P, Chantasrisawad N, Jitsatja A, Ninwattana S, Thippamom N, et al. Dynamics of Neutralizing Antibody and T-Cell Responses to SARS-CoV-2 and Variants of Concern after Primary Immunization with CoronaVac and Booster with BNT162b2 or ChAdOx1 in Health Care Workers. Vaccines (Basel). 2022 Apr;10(5):639. https://doi.org/10.3390/vaccines10050639 PMID:35632395

Supplementary information

File S1. Gating scheme for (A) COOH and (B) SA microspheres.

Supplementary information of this article can be found online at https://polscientific.com/jbm/index.php/jbm/article/view/390/458.